Konrad-Zuse-Zentrum
für Informationstechnik Berlin

Takustraße 7
D-14195 Berlin-Dahlem
Germany

HEIKO SCHMIDT[1] MICHAEL OEVERMANN[2]
ROB J.M. BASTIAANS[3] ALAN R. KERSTEIN[4]

A priori Tabulation of Turbulent Flame Speeds via a Combination of a Stochastic Mixing Model and Flamelet Generated Manifolds[5]

[1]Zuse Institute Berlin (ZIB) and Freie Universität Berlin, Department of Mathematics and Computer Science, e-mail: heischmi@math.fu-berlin.de
[2]Technische Universität Berlin, Institut für Energietechnik, e-mail: michael.oevermann@tu-berlin.de
[3]Eindhoven University of Technology, Mechanical Engineering, The Netherlands, e-mail: r.j.m.bastiaans@tue.nl
[4]Combustion Research Facility, Sandia National Laboratories, Livermore, USA, e-mail: arkerst@sandia.gov
[5]submitted to Flow, Turbulence and Combustion

The work was partially supported by DFG through grant SFB 557/B8 and by the Division of Chemical Sciences, Geosciences, and Biosciences, Office of Basic Energy Sciences, United States Department of Energy, and by the National Science Foundation under Grant No. ATM-0346854.

ZIB-Report 08-02 (Januar 2008)

A priori Tabulation of Turbulent Flame Speeds via a Combination of a Stochastic Mixing Model and Flamelet Generated Manifolds

H. Schmidt, M. Oevermann, R.J.M. Bastiaans, and A.R. Kerstein

January 14, 2008

Abstract

In this paper we propose a technique for *a priori* turbulent flame speed tabulation (TFST) for a given parameter space in standard combustion-regime diagrams. It can be used as a subgrid-scale (SGS) model in Large Eddy Simulation (LES). In a first step, stationary laminar flamelets are computed and stored over the progress variable following the ideas of flamelet generated manifolds (FGM). In a second step, the incompressible one-dimensional Navier-Stokes equations supplemented by the equation for the progress variable are solved on a grid that resolves all turbulent scales. Additionally, turbulent transport is implemented via the linear eddy model (LEM). The turbulent flame structures are solved until a statistically stationary mean value of the turbulent flame speed has been reached. The results are stored in a table that could be used by large scale premixed combustion models, e.g. front tracking schemes. Results are compared to an algebraic model and to direct numerical simulations (DNS).

Keywords: turbulent premixed combustion, flame structures, linear eddy model, flamelet generated manifolds, turbulent burning speed tabulation

Contents

1 Introduction

Due to the interaction between many different time and length scales, turbulent premixed combustion simulation remains a challenging task. Whereas the largest turbulent scales and the slow chemical processes are resolvable, the small scale turbulence/chemistry interaction often has to be modelled. Therefore, the reactive Navier Stokes equations are filtered, dividing the original solution into resolved and unresolved parts, where the latter needs closure. This is commonly done using parameterizations that relate the unresolved parts to the resolved field. For example, the turbulent flame speed, s_t, is an important quantity [13], that is used in many approaches to premixed combustion modeling, e. g., level set methods, flame surface density models, and progress-variable type approaches [4, 14, 20]. There are different possibilities to evaluate this property. The simplest and perhaps least physical is a simple algebraic expression, where often s_t is a function of the unburnt (indicated by subscript u) thermodynamic state and turbulent fluctuations, say

$$s_t = f(u', \boldsymbol{Y}_u, T_u, p_u), \tag{1}$$

where $u', \boldsymbol{Y}, T, p$ are the velocity fluctuation, species mass fraction, temperature and thermodynamic pressure, respectively. Additionally, curvature and stretch effects can be taken into account.

The turbulent flame speed might as well be extracted from stand-alone computations of detailed turbulent flame structures [1, 15].

More recent methods use so-called superparameterizations to determine s_t. Here a one-dimensional microstructure evolution for turbulence chemistry interaction, e.g. [16], is forced by the resolved solution. Suitable integrals over the microstructure yield some of the needed closure terms like the turbulent flame speed. However this procedure is done "online", increasing the costs of such a computation considerably. Even for (stand-alone) one-dimensional calculations of turbulent premixed flames using detailed chemistry and the Linear Eddy Model (LEM [9]) for turbulent transport, the effort is quite high [11, 15].

In this paper, we propose a technique of *a priori* tabulation of s_t for a given reactive setup, e.g., geometric scales, fuel, equivalence ratio, and so on. It can be used as SGS model for LES. The different s_t for the table are computed by evolving one-dimensional turbulent flame structures to a statistically steady state. The steady state assumption is tested with unit root tests and looking at the convergence of the mean. In the flame structure computation we use LEM for the turbulent transport and the idea of Flamelet Generated Manifolds (FGM) [19] for the chemistry tabulation. Both are linked to an implicit solver for the one-dimensional Navier-Stokes equations [8].

As long as the smallest turbulent eddies do not enter the reaction zone, (laminar) chemistry and turbulence can be treated separately. For the chemistry we apply FGM [19] using the code from [11]. In a first step we compute steady one-dimensional laminar flamelets with detailed chemistry and tabulate the flame structure as a function of a suitable progress variables, e. g. CO_2 for a methane air mixture. Additional parameters for tabulation depending on their physical relevance could be stoichiometry, enthalpy, or flame stretch, which changes the laminar burning velocity. In DNS-FGM a correct influence of stretch on the burning velocity was found in Bastiaans et al. [2]. Here stretch effects are not explicitly taken into account.

In the second step we solve the zero Mach number equations for mass, momentum, energy, and progress variable in a one-dimensional domain resolving all spatial and temporal scales. Turbulent advection is implemented using the stochastic LEM. Species mass fractions are uniquely determined by mapping between the progress variable and the pre-calculated FGM of step one. The calculations of step two are performed until a statistically stationary value of s_t has been reached. The extension of our LEM/FGM ansatz to account for stretch effects is currently investigated and will be published elsewhere.
This paper is organized as follows. In the next section, we outline our modeling approach. In section 3 results for turbulent premixed flames for different equivalence ratios and turbulence intensities are presented. These results are compared with currently used algebraic models and DNS. The paper ends with conclusions on the approach and an outlook for further investigations.

2 Model Formulation

Our modeling approach consists of a combination of different stand-alone models, where each model tries to reduce the complexity and cost of turbulent reactive multi-dimensional flow computations. The main steps are (i) constructing a FGM table by computing a sequence of laminar flames to a steady state, (ii) computing a sequence of turbulent flame structures using LEM and the FGM results from (i), (iii) extracting the turbulent burning speed for each run when convergence of the mean is reached, and (iv) building the turbulent data base.

2.1 Flamelet generated manifolds

To make the sequence of turbulent flame structure computations feasible, we apply the flamelet generated manifold (FGM) method [19] to obtain chemical source terms and local mass fraction values. FGM can be considered as a combination of the flamelet approach and the intrinsic low dimensional manifold (ILDM) method [10] and is similar to the flame prolongation of ILDM, FPI, introduced in [6]. FGM is applied similar to ILDM. However, the data base is not generated by applying quasi-steady-state relations for chemical source terms, but by solving a set of one-dimensional convection-diffusion-reaction equations to a steady state of a laminar flame structure. The main advantage of FGM is that diffusion processes, which are important between the preheat zone and the reaction layer, are taken into account. This leads to an accurate method for premixed flames that uses fewer controlling variables than ILDM. The manifold used in this paper is based on a methane/air kinetic mechanism with 16 species and 36 reactions taken from [12]. The extension of the idea to more complicated mechanisms is straightforward [5].
In order to generate the manifolds in step (i), we solve the variable-density zero-Mach-number equations in one spatial dimension on a regular grid. The balance equations for species mass fractions Y_s and temperature T are

$$\rho\frac{\partial Y_s}{\partial t} + \rho u\,\frac{\partial Y_s}{\partial x} = -\frac{\partial j_s}{\partial x} + M_s\,\dot{\omega}_s, \tag{2}$$

$$\rho c_p\frac{\partial T}{\partial t} + \rho u c_p\,\frac{\partial T}{\partial x} = -\frac{\partial q}{\partial x} - \sum_s j_s\,\frac{\partial h_s}{\partial x} - \sum_s h_s\,M_s\,\dot{\omega}_s, \tag{3}$$

with $s = 1, \ldots, n_s$. Here, ρ is the density, u the velocity, j_s the species diffusive flux, M_s the molecular weight of species s, $\dot{\omega}_s$ the chemical source term of species s, c_p the heat capacity at constant pressure, q the heat flux, and h_s the enthalpy of species s including the heat of formation. In the zero-Mach-number limit the pressure is spatially constant and we have a divergence constraint on the velocity

$$\begin{aligned} \frac{\partial u}{\partial x} &= -\frac{1}{\rho c_p T}\left\{\frac{\partial q}{\partial x} + \sum_s j_s \frac{\partial h_s}{\partial x}\right\} \\ &\quad -\frac{1}{\rho}\sum_s \left\{\frac{M}{M_s}\frac{\partial j_s}{\partial x}\right\} + \frac{1}{\rho}\sum_s \left\{\frac{M}{M_s} - \frac{h_s}{c_p T}\right\}\dot{\omega}_s \end{aligned} \tag{4}$$

that can be derived from total energy conservation. Prescribing the inflow velocity at the location x_1 and integrating (4) from $x = x_1$ to $x = x^*$ yields the velocity $u(x = x^*)$. The inflow condition is varied to balance s_t. The density is calculated from the equation of state for an ideal gas $p = \rho T \sum_s Y_s R_s$, where p is the prescribed and spatially constant thermodynamic pressure, T the temperature, and R_s the specific gas constant of species s. The velocity u in eq. (2) and (3) represents the flow velocity induced by dilatational effects due to conduction, and chemical reactions as given by (4).
The zero-Mach-number equations are solved numerically using standard second-order finite-difference discretizations. The time integration of the stiff set of equations is performed using the DAE solver IDA of the SUNDIALS package [8]. Thermodynamic and transport properties as well as reaction rates are calculated using the C++ interface of the CANTERA software package [7]. Diffusion velocities are calculated using a mixture-based formulation with variable Lewis numbers for all species.

2.2 Linear eddy mixing to simulate turbulent transport

In step (ii) of our modeling strategy we solve equations (3) and (4) together with an equation for the progress variable Y_p, here CO_2,

$$\rho\frac{\partial Y_p}{\partial t} + \rho u \frac{\partial Y_p}{\partial x} = -\frac{\partial j_p}{\partial x} + M_p \dot{\omega}_p. \tag{5}$$

The source terms ω_s appearing in (3) and (4) are taken from the FGM tables via interpolation, whereas all thermodynamical properties and mixture based transport coefficients are evaluated using the CANTERA package [7] using the local mass fraction values taken from the FGM.
To extend the concept to the turbulence case we use a stochastic mixing model. In the LEM concept [9], turbulent advection is implemented explicitly by stochastic eddy events. Each eddy event involves a rearrangement of all scalar quantities using so-called 'triplet maps'. The effect of a triplet map is a three-fold compression of the scalar fields in a selected spatial interval whose size is denoted l. This map increases the scalar gradients within the selected interval, analogous to the effect of compressive strain in turbulent flow, without creating discontinuities. Three parameters are needed to implement the eddy events: eddy size l, eddy location within the domain, and the eddy event frequency. The eddy location is randomly sampled from a uniform distribution, and the eddy size is

usually randomly sampled from a given size distribution (e. g., a distribution based on the Kolmogorov inertial-range scaling). The integral length scale l_t and the turbulent diffusivity D_t are the required inputs to the LEM formulation used here. D_t is determined from $D_t = C_D\, l_t u'$ with $C_D = 1/15$ taken from [11, 15, 17, 18]. It is important to note that similar to a DNS, in the LEM concept equations (2) and (3) need to resolve all spatial scales of a turbulent reacting flow.

2.3 The turbulent burning speed

Each coupled LEM/hydrodynamic simulation yields a time series of turbulent premixed methane flame structures. The net mass burning rate is evaluated as an integral over the source terms of the progress variable

$$\rho_u s_t = \frac{1}{Y_{p,\zeta_1} - Y_{p,\zeta_0}} \int_{\zeta_0}^{\zeta_1} \rho \omega_p d\zeta, \tag{6}$$

where ρ_u is the density of the unburnt mixture, ζ is the one-dimensional coordinate and ω_p denotes the source term of the progress variable Y_p. Hence, the outcome of each LEM run is a time series $s_t(t)$. From this series one could construct the pdf of s_t for the given turbulence level and composition. Therefore one has to check for strong convergence, whereas for a steady mean value and variation, only weak convergence is required. Here, we focus on the latter. Whether one has fast or slow convergence depends strongly on the studied process. If the pdf is near Gaussian, it is reached much faster than for, e.g., burning speeds of flames in the thin reaction zone regime, where a typical pdf(s_t) is far from being Gaussian. Here, the runs are stopped when the mean converges.

3 Results and Discussion

In this section we give an example of how to build a data base for the turbulent flame speed that later might be used by, e.g., a level-set front-tracking scheme or any other numerical method for premixed turbulent combustion using s_t. We illustrate the main steps, namely (i) constructing a FGM table by computing a sequence of laminar flames to a steady state, (ii) computing a sequence of turbulent flame structures using LEM with a progress variable approach using the FGM results, (iii) extracting the turbulent burning speed for each run when (at least) weak statistical convergence is reached, and (iv) building the turbulent data base. First qualitative and quantitative comparisons with algebraic models and DNS are carried out.

3.1 The FGM tabulation

In Figure 1 the tabulated chemical source term of the progress variable CO_2 using the chemical reaction mechanism for CH_4 combustion from Peters [12] is plotted as a function of the progress variable and equivalence ratio ϕ ranging from lean to stoichiometric conditions ($\phi = 1$). The source terms of all other variables are stored as well. Some results of laminar flame properties obtained with the model are summarized in Table 1.

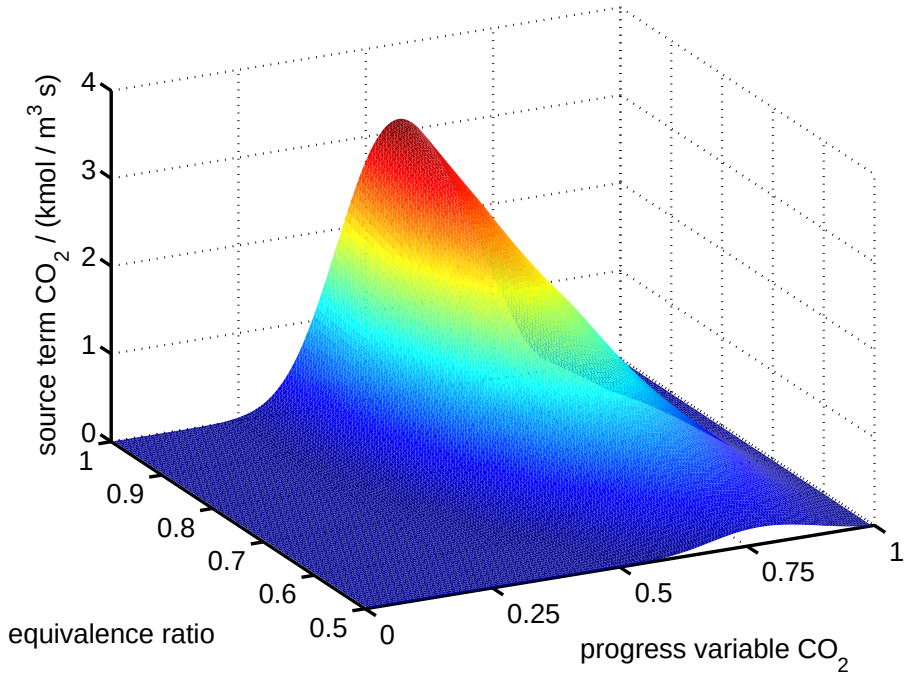

Figure 1: Tabulated source term of the progress variable, CO_2, plotted over the equivalence ratio and the CO_2 mass fraction. Methane/air chemistry is used.

$\phi[-]$	0.5	0.6	0.7	0.8	0.9	1.0
l_F[mm]	1.348	0.746	0.556	0.478	0.449	0.442
s_l[cm/s]	6.57	14.11	21.60	27.81	31.97	33.63

Table 1: Laminar flame thickness (l_F) and the laminar burning speed (s_l) for different equivalence ratios ϕ.

3.2 Turbulent flame structures

In the second step we use the FGM generated source terms as an input for the LEM computations of the turbulent flame structures. This approach reduces the number of species within the LEM module to the number of progress variables of the FGM and allows a fast computation over a large parameter space. Here we use CO_2 as progress variable. Some snapshots of a calculated turbulent methane/air flame structure for $\phi = 0.8$, $l_t = 5$mm, and $u' = 0.6$m/s are plotted in Figure 2 (main species) and Figure 3 (minor species).

3.3 The extracted turbulent burning speed and statistical convergence

From each flame structure we extract the turbulent burning speed via equation (6). A typical time history of s_t is plotted in Figure 4. The mean value of s_t in

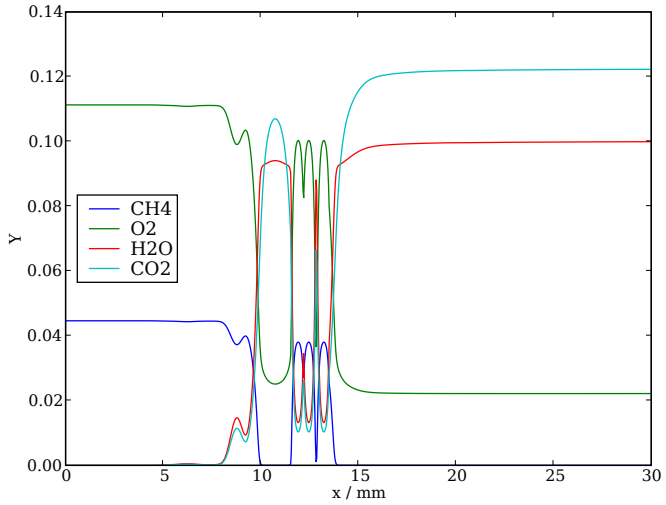

Figure 2: Snapshot of the major species of the turbulent methane flame for $\phi = 0.8$, $l_t = 5$mm, and $u' = 0.6$m/s

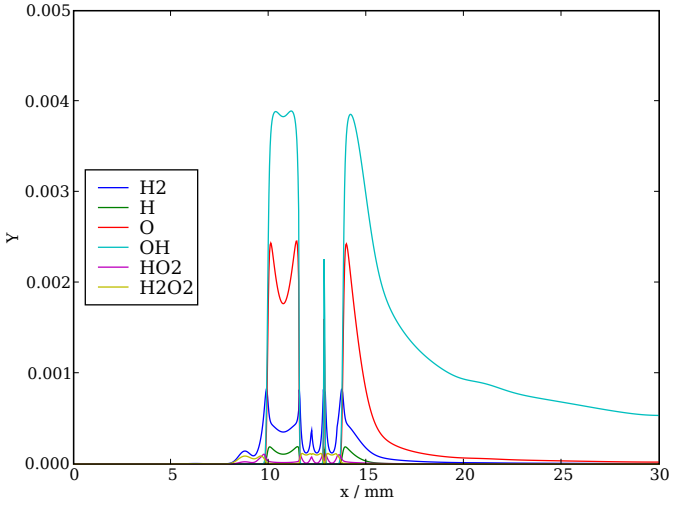

Figure 3: Snapshot of the minor species of the turbulent methane flame for $\phi = 0.8$, $l_t = 5$mm, and $u' = 0.6$m/s

Figure 5 indicates that we have not reached a statistically steady state yet. To obtain strong statistical convergence, one has to wait until the whole pdf of s_t is converged. Here, we stop the computations when the first moment is converged to a steady state. This constraint is even less than is normally meant by weak statistical convergence which requires convergence of mean and variance. But,

it can be concluded from Figure 6 that, even to get convergence of the mean of s_t, it is necessary to calculate over a time interval that is quite large compared to the integral eddy turn over time. For the different set-ups, the factor ranges from about 20 to 200. Generally, this is a much longer time than standard DNS cases are run for, but DNS runs may be less intermittent compared to our LEM simulations. A run over a longer time interval is shown for a different case in Figure 6.

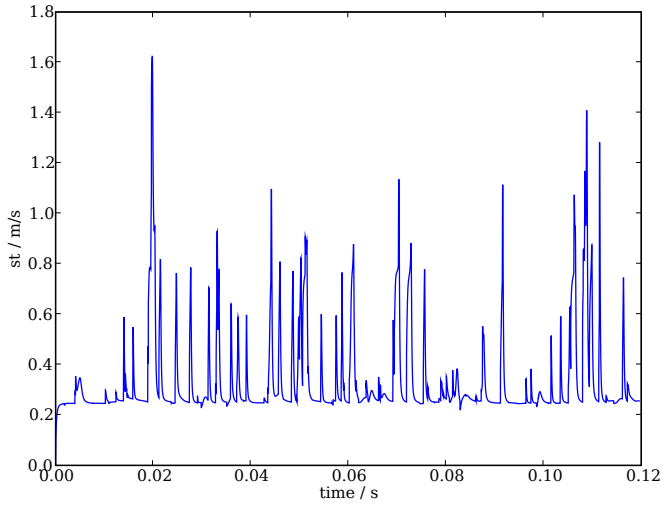

Figure 4: Time history of the turbulent burning velocity for the case $\phi = 0.7$, $l_t = 5$mm, and $u' = 0.6$m/s

To check the tabulated results we redo a calculation using detailed chemistry. A comparison of the two time evolutions for the turbulent burning velocity are plotted in Figure 7. The comparison is quite good. especially for the mean value of s_t.

3.4 A data base for the turbulent burning velocity

To construct a data base of s_t values, we repeat the turbulent flame structure computations for different turbulent fluctuations and equivalence ratios. Our tabulation region is shown in the well known Borghi diagram, see Figure 8.

The exact coordinates of the computations which depend in our example on stoichiometry and turbulence conditions are summarized in Table 2.

The results for the mean turbulent burning speed are shown in Table 3 and the interpolated manifold is plotted in Figure 9.

The interpolated s_t shows a monotonic behaviour. Highest values are reached for the stoichiometric flame at the highest turbulence intensity. For lean mixtures changes in turbulence levels have a smaller effect than for richer flames. This can be explained by the different laminar flame thicknesses and the associated change in combustion regime.

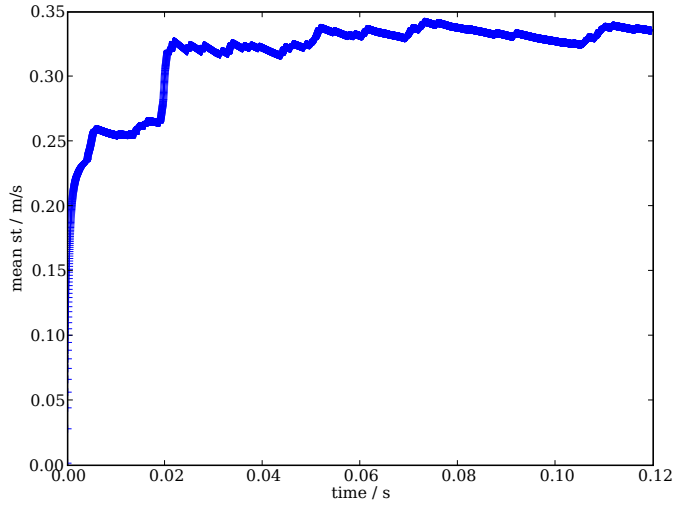

Figure 5: Time history of the mean turbulent burning velocity for the case $\phi = 0.7$, $l_t = 5$mm, and $u' = 0.6$m/s

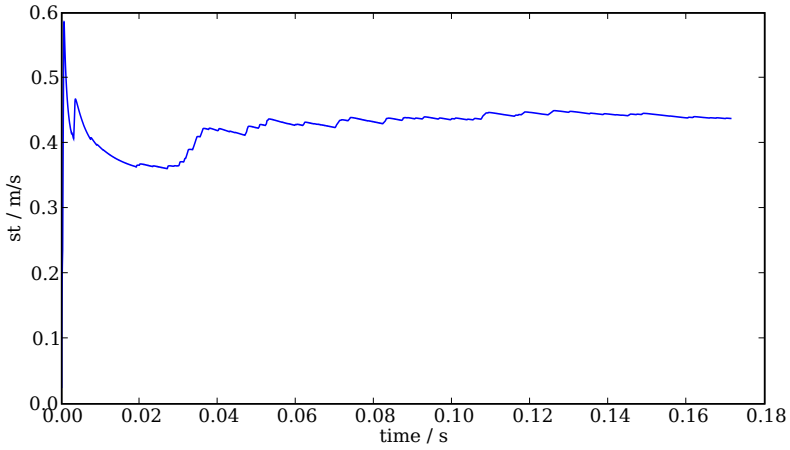

Figure 6: Time history of the mean turbulent burning velocity for the case $\phi = 0.9$, $l_t = 5$mm, and $u' = 0.6$m/s

3.5 TFST vs. an algebraic model

A first quantitative test for our new TFST idea is the comparison of our turbulent flame speed results with an algebraic model. We consider the turbulent flame speed model from [4] which has the following form:

$$s_t = s_l \left(1 + \min\left[\frac{\Delta}{l_F}, \Gamma \frac{u'_\Delta}{s_l}\right]\right)^\beta. \tag{7}$$

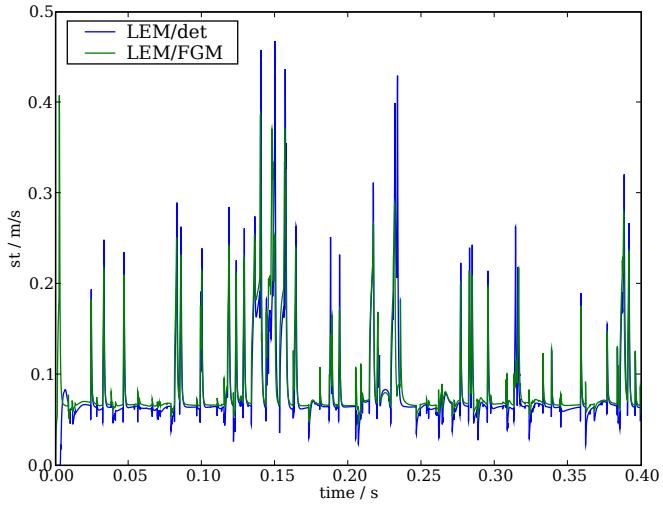

Figure 7: Time evolution of the turbulent flame speed for detailed and tabulated chemistry for the same initial conditions

$u'\backslash\phi$	0.5	0.6	0.7	0.8	0.9	1.0
0.33	5.02;3.71	2.34;6.7	1.53;8.99	1.19;10.46	1.03;11.14	0.98;11.31
0.66	10.04;3.71	4.68;6.7	3.06;8.99	2.37;10.46	2.06;11.14	1.96;11.31
0.99	15.07;3.71	7.02;6.7	4.58;8.99	3.56;10.46	3.10;11.14	2.94;11.31
1.30	19.79;3.71	9.21;6.7	6.02;8.99	4.67;10.46	4.07;11.14	3.87;11.31

Table 2: Coordinates (y; x) = $u'/s_l; l_t/l_F$ in the Borghi diagram for the cases considered

u'[cm/s] \ ϕ	0.5	0.6	0.7	0.8	0.9	1.0
0.33	8.62	17.28	29.02	33.50	38,59	38,65
0.66	9.28	20.95	27.23	38.34	42.53	43,52
0.99	9.70	22.45	37.29	45,32	48.01	50,82
1.30	10.94	23.72	40.32	45.94	53.72	56.75

Table 3: The mean turbulent burning speed, s_t, as a function of stoichiometry and velocity fluctuations for the different calculations

Here we set the filter size Δ to the integral turbulent length scales of the different runs and u'_Δ to the integral velocity fluctuations. The laminar burning velocities and the flame laminar thickness l_F are taken from the laminar flame calculations. Γ is an efficiency function defined in [4] and β a parameter associated with the fractal dimension of the turbulent flame surface. In Table 4 the results for the considered turbulence intensities and stoichiometry are shown for $\beta = 0.23$ which gives a fractal dimension of 2.23. The same results are summarized in Table 5 for $\beta = 0.5$. In Figure 10 and Figure 11 the algebraic and TFST

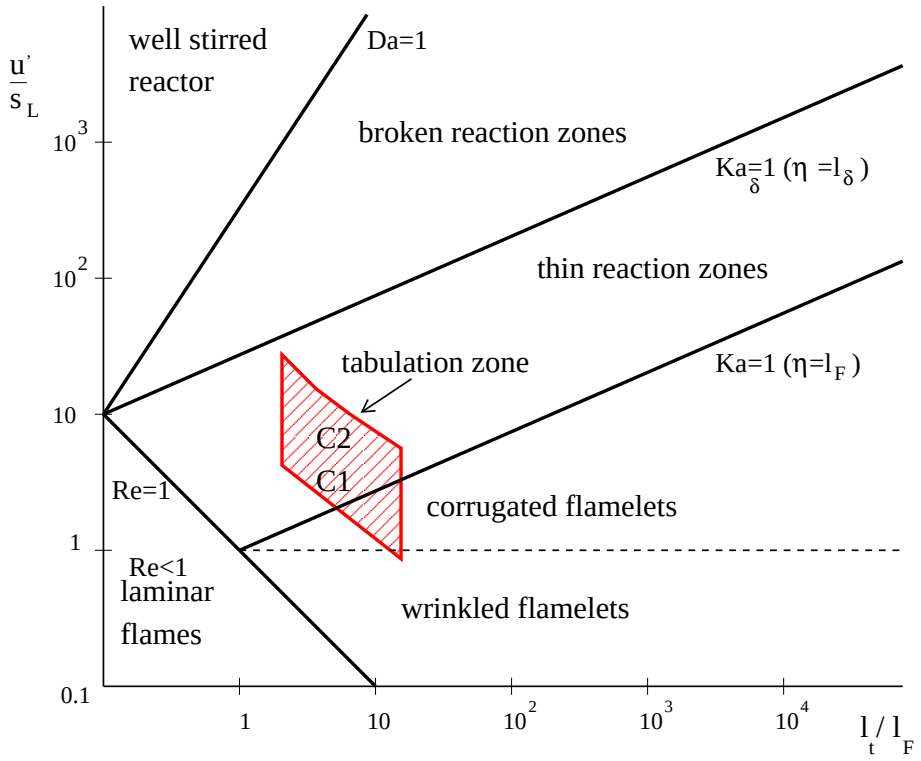

Figure 8: Diagram of turbulence/chemistry regimes. Conditions C1 and C2 are discussed in section 3.6. $Re = l_t u'/\nu$ ist the turbulent Reynolds number, where ν is the kinematic viscosity, l_t is the scale of the biggest turbulent eddies, and u' is a typical velocity fluctuation. $Ka = l_F^2/\eta^2$ ist the Karlovitz number, where η is the size of the smallest turbulent eddies and l_F is the flame thickness. Another Karlovitz number $Ka_\delta = l_\delta^2/\eta^2$ is defined with the reaction zone thickness l_δ.

u'[cm/s] \ ϕ	0.5	0.6	0.7	0.8	0.9	1.0
0.33	9.38	19.9	27.0	33.0	36.60	38.10
0.66	9.38	22.6	34.1	41.0	45.20	46.80
0.99	9.38	22.6	36.7	46.9	51.8	53.60
1.30	9.38	22.6	36.7	48.7	55.2	57.2

Table 4: The mean turbulent burning speed, s_t given by the algebraic model of Charlette for $\beta = 0.23$

results are plotted over the parameter range under investigation. Whereas the agreement for the $\beta = 0.23$ case is quite good in the entire region, the results deviate from each other quite considerably for the $\beta = 0.5$ case- at least in the high turbulence stiochiometric regions. In this limit an order one difference between the two models is observed. This illustrates the importance of the choice of the fractal dimension in the algebraic model. In the future it might be possible that our method helps to find reasonable choices for β depending on

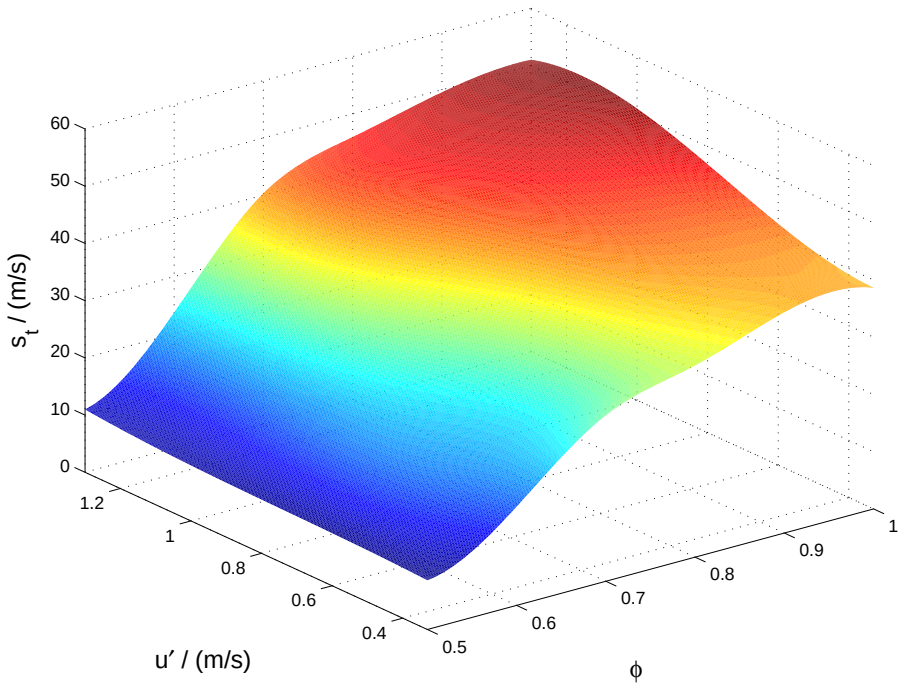

Figure 9: Tabulated turbulent burning speed as a function of stoichiometry and velocity fluctuations

u'[cm/s] \ ϕ	0.5	0.6	0.7	0.8	0.9	1.0
0.33	14.3	29.9	36.1	40.30	43.00	44.10
0.66	14.3	39.2	58.4	64.6	67.80	68.90
0.99	14.3	39.2	68.3	86.6	91.3	92.80
1.30	14.3	39.2	68.3	94.1	105.9	107.0

Table 5: The mean turbulent burning speed, s_t given by the algebraic model of Charlette for $\beta = 0.5$

local turbulence/chemistry conditions.

3.6 Comparison with DNS results

While the first comparison was rather of qualitative nature, the following step is to check our results quantitatively against DNS. A statistically flat flame might be seen as an elementary small scale building block of a turbulent premixed flame. Swart et al. [5] investigate turbulent flame speeds with a DNS resolved flow field while using FGM for the chemical kinetics. The two configurations shown in Figure 8, named like in the original article $C1$ and $C2$, lie in our tabulation zone. Therefore they are a good check for our turbulent flame speed results. The comparison is found in Table 6. The observed discrepancy between TFST and DNS results is less than 7%.

A second comparison is performed with another DNS of a freely propagating

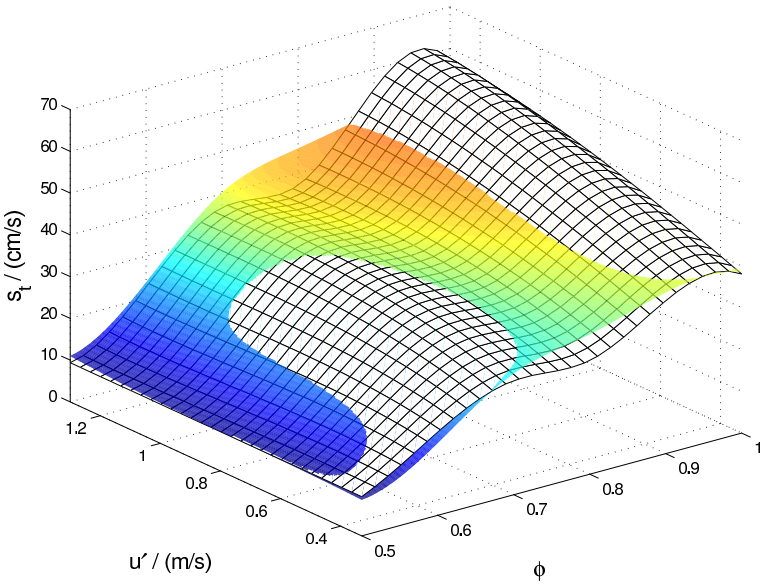

Figure 10: The turbulent burning speed s_t given by the algebraic model of Charlette for $\beta = 0.23$ (mesh) compared to TFST from Figure 9

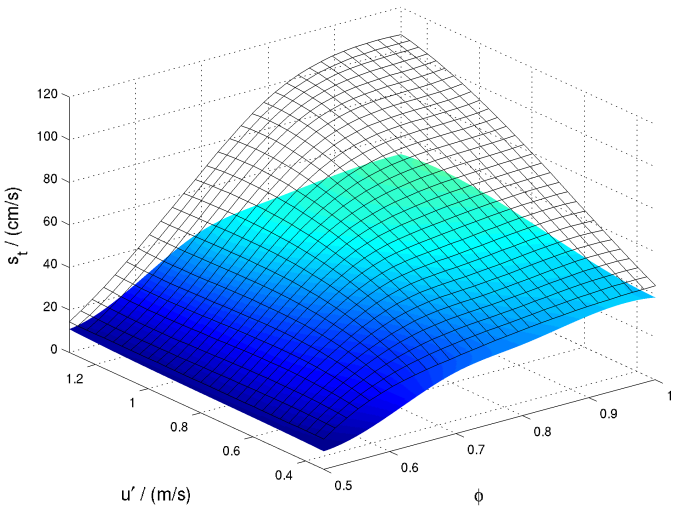

Figure 11: The turbulent burning speed s_t given by the algebraic model of Charlette for $\beta = 0.5$ (mesh) compared to TFST from Figure 9

flame taken from Chakraborty and Cant [3]. In the DNS a one step Arrhenius kinetic is used for the chemistry. TFST results are shown in Table 7 and compared to DNS (case F of their paper) for equivalent non dimensional numbers relating turbulence and chemistry. The error margin is comparable to the first DNS case.

	C1 TFST	C2 TFST	C1 DNS	C2 DNS
l_t[mm]	2.78	2.78	2.78	2.78
l_F[mm]	0.556	0.556	0.556	0.556
$l_t/l_F[-]$	5.0	5.0	5.0	5.0
u'[m/s]	0.7	1.4	0.7	1.38
s_l[m/s]	0.216	0.216	0.213	0.213
$u'/s_l[-]$	3.3	6.5	3.3	6.5
$s_t/s_l[-]$	1,21	1.32	1.13	1.39

Table 6: Parameters and relations for DNS and TFST simulations

	DNS Case F	TFST Case F
$l_t/l_F[-]$	4.05	4.05
$u'/s_l[-]$	7.62	7.62
$s_t/s_l[-]$	2.0	1.85

Table 7: Non dimensional relations for DNS and TFST simulations

4 Summary and Outlook

A technique of an *a priori* turbulent flame speed tabulation (TFST) for a chosen parameter space is presented. In a first step, stationary laminar flamelets are computed and stored over a chosen progress variable following the ideas of flamelet generated manifolds (FGM). In a second step, the incompressible one-dimensional Navier-Stokes equations supplemented by the equation for the progress variable are solved on a grid that resolves all turbulent and chemical scales. In addition, turbulent transport is implemented via the linear eddy model (LEM). The turbulent flame structures are solved until a statistically stationary state for the mean flame speed is reached. The time for convergence is quite high compared with eddy turnover times. This is due to the fact that statistically rare events, like the big turbulent eddies, have a major impact on the flame structure and the burning speed. Only after a higher number of these events the mean value does converge. The results are stored in a table that could be used by large scale premixed combustion models, e.g. front tracking schemes.

We compare results of our method with a recent algebraic model for turbulent flame speed and DNS results. The agreement is quite reasonable, especially the comparative results with the DNS.

In the future, the idea can easily be extended to other parametric dependencies of the turbulent burning speed. This could be, e.g, stretch, curvature, and integral length scale effects. Our strategy could also be applied for building a pdf of subgrid scale (SGS) s_t values which could then be used in large eddy simulations (LES). The pdf can be built by averaging the LEM solutions over time intervals corresponding to LES time steps. Finally, the LES samples the s_t values from the constructed pdf. Justification of this procedure would require further investigation of the intermittent behavior discussed in Sec. 3.3.

Acknowledgement

This work was partially supported by the Division of Chemical Sciences, Geosciences, and Biosciences, Office of Basic Energy Sciences, United States Department of Energy, and by the National Science Foundation under Grant No. ATM-0346854. Sandia National Laboratories is a multi-program laboratory operated by Sandia Corporation, a Lockheed Martin Company, for the United States Department of Energy under contract DE-AC04-94-AL85000. H. S. thanks the Deutsche Forschungsgemeinschaft (DFG) for partially supporting this work through grant SFB 557/B8. The authors gratefully acknowledge fruitful, stimulating discussions with J. A. van Oijen and L. P. H. de Goey.

References

[1] M.S. Anand and S.B. Pope. Calculations of premixed turbulent flames by pdf methods. *Combustion and Flame*, 67:127–142, 1987.

[2] R.J.M. Bastiaans, J.A. van Oijen, and L.P.H. de Goey. Application of flamelet generated manifolds and flamelet analysis of turbulent combustion. *Int. Jnl. Multiscale Comp. Eng.4(3), 307-317, (2006)*, 4(3):307–317, 2006.

[3] N. Chakraborty and R. S. Cant. Effects of strain rate and curvature on surface density function transport in turbulent premixed flames in the thin reaction zones regime. *Physics of Fluids*, 17:065108, 2005.

[4] F. Charlette, C. Meneveau, and D. Veynante. A power-law flame wrinkling model for LES of premixed turbulent combustion Part II: Dynamic formulation. *Combustion and Flame*, 131:181–197, 2002.

[5] J.A.M. de Swart, R.J.M. Bastiaans, J.A. van Oijen, and L.P.H de Goey. Turbulent burning rates from DNS of lean, statistically flat methane flames. In *Proc. of the European Combustion Meeting 2007, Chania, Crete*, 2007.

[6] O. Gicquel, N. Darabiha, and D. Thevenin. *Proceedings of the Combustion Institute*, 28:1901–1908, 2000.

[7] D. Godwin. Cantera: Object-oriented software for reacting flows. http://www.cantera.org.

[8] A. C. Hindmarsh. Sundials: Suite of nonlinear and differential/algebraic equation solvers. Technical report, UCRL-JRNL-200037, Lawrence Livermore National Laboratory, 2004.

[9] A. R. Kerstein. Linear-eddy model of turbulent transport and mixing. *Combustion Science and Techology*, 60:391–421, 1988.

[10] U. Maas and S. B. Pope. Simplifying chemical kinetics: Intrinsic low-dimensional manifolds in composition space. *Combustion and Flame*, 88:239–264, 1992.

[11] M. Oevermann, H. Schmidt, and A. R. Kerstein. Linear eddy modelling of auto-ignition under thermal stratification with application to HCCI engines. In *Third European Combustion Meeting (ECM2007), Chania, Crete*, 2007.

[12] N. Peters. Fifteen lectures on laminar and turbulent combustion. Technical report, Ercoftac Summer School, RWTH Aachen, 1996.

[13] N. Peters. The turbulent burning velocity for large scale and small scale turbulence. *Journal of Fluid Mechanics*, 384:197–132, 1999.

[14] N. Peters. *Turbulent Combustion*. Cambridge University Press, 2000.

[15] V. Sankaran and Menon. S. Structure of premixed turbulent flames in the thin-reaction-zones regime. *Proceedings of the Combustion Institute*, 28:203–209, 2000.

[16] H. Schmidt and R. Klein. A generalized level-set/in-cell-reconstruction approach for accelerating turbulent premixed flames. *Combustion Theory and Modelling*, 7:243–267, 2003.

[17] T. Smith and S. Menon. Model simulations of freely propagating turbulent premixed flames. In *Proceedings of the Combustion Institute*, 1996.

[18] T. Smith and S. Menon. One-dimensional simulations of freely propagating turbulent premixed flames. *Combustion Science and Technology*, 128:99–130, 1997.

[19] J. A. van Oijen and L. P. H. de Goey. Modelling of premixed laminar flames using flamelet-generated manifolds. *Combustion Science and Technology*, 161:113–137, 2000.

[20] V. L. Zimont and A. N. Lipatnikov. A numerical model of premixed turbulent combustion of gases. *Chemical Physics Reports*, 14:993–1025, 1995.